Stepwise Conversion of an Osmium Trimethylstannyl Complex to a Triiodostannyl Complex and Nucleophilic Substitution Reactions at the Tin−Iodine Bonds

Alex M. Clark, Clifton E. F. Rickard, Warren R. Roper,* Timothy J. Woodman, and L. James Wright*

Department of Chemistry, The University of Auckland, Private Bag 92019, Auckland, New Zealand

Received November 15, 1999

Treatment of the coordinatively unsaturated osmium complex $Os(SnMe_3)Cl(CO)(PPh_3)_2$ with sodium dimethyldithiocarbamate gives the coordinatively saturated complex $Os(SnMe_3)(\eta^2\text{-}S_2CNMe_2)(CO)(PPh_3)_2$ (**1**). Complex **1** reacts with excess SnI_4 to give $Os(SnMeI_2)(\eta^2\text{-}S_2CNMe_2)(CO)(PPh_3)_2$ (**3**) in high yield. A redistribution reaction of **3** with an equimolar amount of **1** provides $Os(SnMe_2I)(\eta^2\text{-}S_2CNMe_2)(CO)(PPh_3)_2$ (**2**). The last remaining methyl group bonded to tin in **3** is removed by treatment with a slight excess of I_2, giving the triiodostannyl complex $Os(SnI_3)(\eta^2\text{-}S_2CNMe_2)(CO)(PPh_3)_2$ (**4**). Both **3** and **4** have been further derivatized by replacement of the halide groups on tin. Treatment of **3** with pyridinium tribromide gives $Os(SnMeBr_2)(\eta^2\text{-}S_2CNMe_2)(CO)(PPh_3)_2$ (**5**). Treatment of **3** with catechol provides $Os(SnMe[1,2\text{-}O_2C_6H_4])(\eta^2\text{-}S_2CNMe_2)(CO)(PPh_3)_2$ (**6**), while the similar reaction with 1,2-ethanedithiol gives $Os(SnMe[1,2\text{-}S_2C_2H_4])(\eta^2\text{-}S_2CNMe_2)(CO)(PPh_3)_2$ (**7**). Complex **4** undergoes reaction with an excess of KOH to give the trihydroxystannyl complex $Os(Sn[OH]_3)(\eta^2\text{-}S_2CNMe_2)(CO)(PPh_3)_2$ (**8**). Treatment of **4** with triethanolamine gives $Os(Sn[OCH_2CH_2]_3N)(\eta^2\text{-}S_2CNMe_2)(CO)(PPh_3)_2$ (**9**), while reaction with nitrilotriacetic acid gives the metal-substituted stannatranone $Os(Sn[OC(O)CH_2]_3N)(\eta^2\text{-}S_2CNMe_2)(CO)(PPh_3)_2$ (**10**). The crystal structures of **1**, **4**, **5**, **7**, and **10** have been determined.

Introduction

Transition metal stannyl complexes L_nM-SnR_3 are widely represented in the literature.[1] These complexes are interesting because of the variety of reactions that they may undergo, including (i) ligand substitution at the transition metal center, (ii) cleavage of the organo groups from the tin donor atom by electrophilic reagents such as halogens or hydrogen halides, and (iii) nucleophilic substitution of good leaving groups at the tin center to afford stannyl complexes with novel functionalities.[2]

We have previously described the synthesis of coordinatively unsaturated osmium and ruthenium stannyl complexes $M(SnR_3)Cl(CO)(PPh_3)_2$ (M = Ru; R = Me, *n*-butyl, *p*-tolyl; M = Os; R = Me) and the subsequent elaboration of these complexes at the transition metal center.[3,4] We have also shown that when halide substituents are introduced at the tin center, further reactions are possible, and novel derivatives such as the monomeric thiahydroxystannyl complex $Ru(SnMe_2SH)I(CO)(CN[p\text{-tolyl}])(PPh_3)_2$ may be prepared.[5] Furthermore, in a recent preliminary communication,[6] we described the synthesis of the first metal-bound stannatrane through reaction between $Os(SnI_3)(\eta^2\text{-}S_2CNMe_2)(CO)(PPh_3)_2$ and triethanolamine.[6] Herein we report in full the stepwise introduction of halo substituents into $Os(SnMe_3)(\eta^2\text{-}S_2CNMe_2)(CO)(PPh_3)_2$ and the further derivatization reactions of these complexes to afford stannyl ligands with a range of unusual functionalities.

Results and Discussion

Selective Cleavage of Organo Groups from the Tin Center. Redistribution reactions of SnX_4 with SnR_4, in appropriate stoichiometries, provides a general route to SnR_xX_{4-x} compounds (Kocheshkov disproportionation[7]). We have used this approach in derivatization of the transition metal-substituted organotin compound $Os(SnMe_3)(\eta^2\text{-}S_2CNMe_2)(CO)(PPh_3)_2$ (**1**). $Os(SnMe_3)(\eta^2\text{-}S_2CNMe_2)(CO)(PPh_3)_2$ (**1**) is synthesized by

(1) (a) Mackay, K. M.; Nicholson, B. K. In *Comprehensive Organometallic Chemistry*; Wilkinson, G., Stone, F. G. A., Abel, E. W., Eds.; Pergamon Press: New York, 1982; Vol. 2, pp 1043−1114. (b) Petz, W. *Chem. Rev.* **1986**, *86*, 1019. (c) Holt, M. S.; Wilson, W. L.; Nelson, J. H. *Chem. Rev.* **1989**, *89*, 11. (d) Lappert, M. F.; Rowe, R. S. *Coord. Chem. Rev.* **1990**, *100*, 267.

(2) (a) Aylett, B. J. *Organometallic Compounds, Part Two; Groups IV and V*; Chapman and Hall: London, 1979; p 274, and references therein. (b) Bichler, R. E. J.; Clark, H. C.; Hunter, B. K.; Rake, A. T. *J. Organomet. Chem.* **1974**, *69*, 367. (c) Booth, M. R.; Cardin, D. J.; Carey, N. A. D.; Clark, H. C.; Sreenathan, J. *J. Organomet. Chem.* **1970**, *21*, 171. (d) Chipperfield, J. R.; Clark, S.; Webster, D. E.; Yusof, H. *J. Organomet. Chem.* **1991**, *421*, 205. (e) Roberts, R. M. G. *J. Organomet. Chem.* **1973**, *47*, 359. (f) Lappert, M. F.; McGeary, M. J.; Parish, R. V. *J. Organomet. Chem.* **1989**, *373*, 107. (g) Powell, P. *Inorg. Chem.* **1968**, *7*, 2458.

(3) Clark, G. R.; Flower, K. R.; Roper, W. R.; Wright, L. J. *Organometallics* **1993**, *12*, 259.

(4) Craig, P. R.; Flower, K. R.; Roper, W. R.; Wright, L. J. *Inorg. Chim. Acta* **1995**, *240*, 385.

(5) Clark, G. R.; Flower, K. R.; Roper, W. R.; Wright, L. J. *Organometallics* **1993**, *12*, 3810.

(6) Rickard, C. E. F.; Roper, W. R.; Woodman, T. J.; Wright, L. J. *Chem. Commun.* **1999**, 837.

(7) Kocheshkov, K. A. *Ber.* **1926**, *62*, 996.

10.1021/om990904x CCC: $19.00
Publication on Web 04/06/2000

Scheme 1

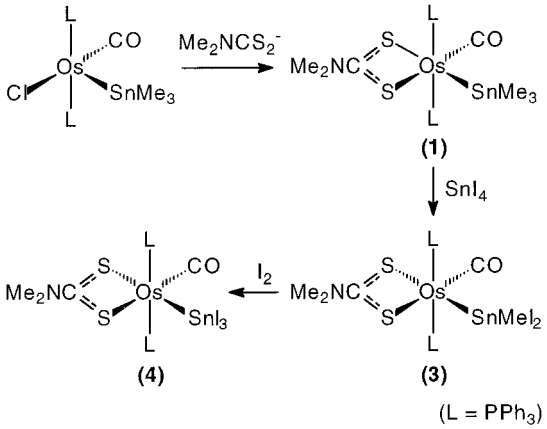

Scheme 2

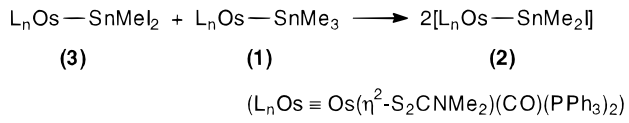

the addition of NaS_2CNMe_2 to the coordinatively unsaturated osmium complex $Os(SnMe_3)Cl(CO)(PPh_3)_2$.[4] Compound **1** proves to be an excellent starting point for investigating derivatization reactions at tin since all the ancillary ligands bound to the transition metal center are resistant to substitution, with the result that the metal ligand fragment "$Os(\eta^2\text{-}S_2CNMe_2)(CO)(PPh_3)_2$" behaves as a single, unreactive, bulky, functional group on tin. While attempts to cleave the methyl groups from tin in complex **1** directly through reaction with I_2 in dichloromethane were only partially successful with significant Os−Sn bond cleavage occurring, it was found that treatment of **1** with an excess of SnI_4 in benzene provides yellow $Os(SnMeI_2)(\eta^2\text{-}S_2CNMe_2)(CO)(PPh_3)_2$ (**3**) in high yield (see Scheme 1). In contrast to the reaction with I_2 there is no evidence for any cleavage of the osmium−tin bond. Variation of the reaction conditions, e.g., elevated temperatures or higher proportions of SnI_4, failed to provide any product other than **3**; in particular no triiodostannyl products were detected. However, the last methyl group in **3** could be replaced by treatment with an equivalent amount of I_2, providing $Os(SnI_3)(\eta^2\text{-}S_2CNMe_2)(CO)(PPh_3)_2$ (**4**) in high yield. It should be noted that unlike **1**, reaction of **3** with I_2 did not result in cleavage of the Os−Sn bond, presumably because the two electron-withdrawing iodo substituents on tin decreased the susceptibility of the Os−Sn bond toward electrophilic attack. In a further demonstration of the viability of redistribution reactions taking place on metal-bound tin ligands, reaction of **2** with 1 equiv of $Os(SnMe_3)(\eta^2\text{-}S_2CNMe_2)(CO)(PPh_3)_2$ (**1**) in benzene at 45 °C provides a convenient synthetic pathway to $Os(SnMe_2I)(\eta^2\text{-}S_2CNMe_2)(CO)(PPh_3)_2$ (**2**) (see Scheme 2).

Complexes **1**, **2**, **3**, and **4** have been fully characterized by a range of spectroscopic techniques, and for **1** and **4** crystal structure analyses have been completed (see below). The IR spectra of **1**−**4** all show similar features (see Table 1). As expected, the ν(CO) bands shift to higher wavenumbers with increasing halide substitution; that is, for **1**−**4** ν(CO) is at 1859, 1914, 1927, and 1936 cm^{-1}, respectively. In each spectrum the dithiocarbamate ligand is apparent from absorptions near

Scheme 3

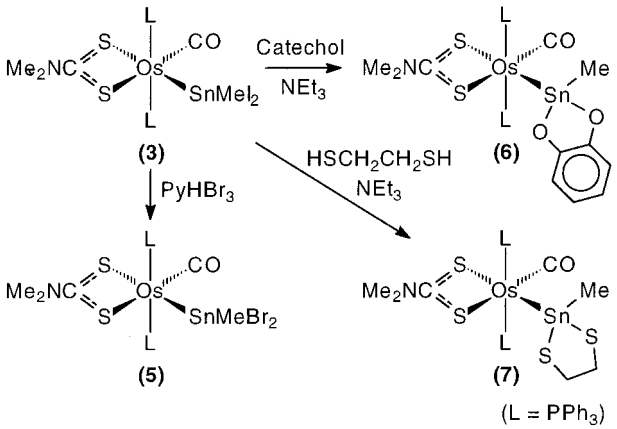

Scheme 4

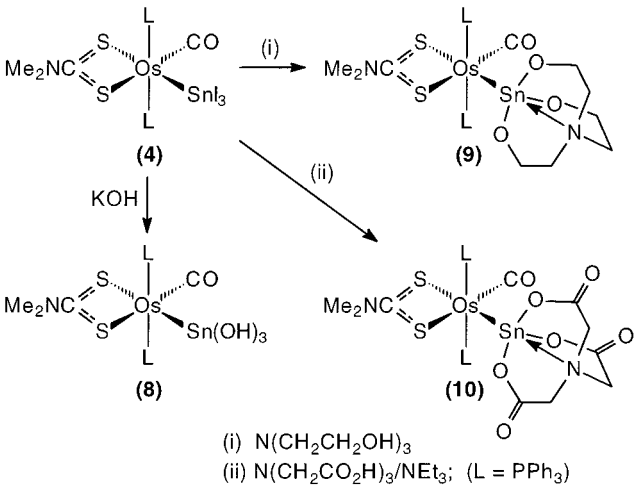

1535 and 1160 cm^{-1}. A similar trend is clearly discernible for the positions of the methyl proton resonances in the ^1H NMR spectra, with chemical shifts moving to lower field values as the degree of iodine substitution at tin increases (see Table 2).

Reactions at Tin in $Os(SnMeI_2)(\eta^2\text{-}S_2CNMe_2)(CO)(PPh_3)_2$ (3) (see Scheme 3). Tin halides are susceptible to nucleophilic substitution, and reactions of this type can lead to a variety of new tin derivatives.[8,9] Among these products, those with group 16 element−tin bonds have received much attention. Those with hydroxy, thiahydroxy, and selenahydroxy functionalities tend to form polymeric structures following condensation reactions. The steric protection afforded by bulky aromatic groups has allowed at least one monomeric stannahydroxy compound to be isolated,[10] and we have previously described the monomeric thiastannyl complex $Ru(SnMe_2SH)I(CO)(CN\textit{p}\text{-tolyl})(PPh_3)_2$,[5] which is stabilized at least in part by the large triphenylphosphine ligands. $Os(SnMeI_2)(\eta^2\text{-}S_2CNMe_2)(CO)(PPh_3)_2$, with two halide substituents on tin, has the potential to react

(8) (a) Davies, A. G. *Organotin Chemistry*; VCH: Weinheim, 1997. (b) Davies, A. G.; Smith, P. J. In *Comprehensive Organometallic Chemistry*; Wilkinson, G., Stone, F. G. A., Abel, E. W., Eds.; Pergamon Press: New York, 1982; Vol. 2, pp 519−627.

(9) (a) Puff, H.; Reuter, H. *J. Organomet. Chem.* **1989**, *364*, 57. (b) Puff, H.; Reuter, H. *J. Organomet. Chem.* **1989**, *368*, 173. (c) Puff, H.; Reuter, H. *J. Organomet. Chem.* **1989**, *373*, 173. (d) Reuter, H.; Puff, H. *J. Organomet. Chem.* **1989**, *379*, 223.

(10) Vicente, J.; Chicote, M.-T.; Ramírez-de-Arellono, M. del-C.; Jones, P. G. *J. Chem. Soc., Dalton Trans.* **1992**, 1839.

Table 1. Infrared Data (cm^{-1})[a] for Osmium Stannyl Complexes

complex	ν(C=O)	(S_2CNMe_2)	other bands
$Os(SnMe_3)(\eta^2\text{-}S_2CNMe_2)(CO)(PPh_3)_2$ (**1**)	1859	1518, 1157	
$Os(SnMe_2I)(\eta^2\text{-}S_2CNMe_2)(CO)(PPh_3)_2$ (**2**)	1914	1531, 1157	
$Os(SnMeI_2)(\eta^2\text{-}S_2CNMe_2)(CO)(PPh_3)_2$ (**3**)	1927	1537, 1161	
$Os(SnI_3)(\eta^2\text{-}S_2CNMe_2)(CO)(PPh_3)_2$ (**4**)	1936	1538, 1161	
$Os(SnMeBr_2)(\eta^2\text{-}S_2CNMe_2)(CO)(PPh_3)_2$ (**5**)	1914	1532, 1156	
$Os(SnMe[\eta^2\text{-}O_2C_6H_4])(\eta^2\text{-}S_2CNMe_2)(CO)(PPh_3)_2$ (**6**)	1910	1526, 1159	1246,[b] 1092[b]
$Os(SnMe[SCH_2CH_2S])(\eta^2\text{-}S_2CNMe_2)(CO)(PPh_3)_2$ (**7**)	1907	1519, 1153	
$Os(Sn[OH]_3)(\eta^2\text{-}S_2CNMe_2)(CO)(PPh_3)_2$ (**8**)	1916	1534, 1158	3400,[c] 1640[c]
$Os(Sn[OCH_2CH_2]_3N)(\eta^2\text{-}S_2CNMe_2)(CO)(PPh_3)_2$ (**9**)	1896	1155	
$Os(Sn\ [OC(O)CH_2]_3N)(\eta^2\text{-}S_2CNMe_2)(CO)(PPh_3)_2$ (**10**)	1920	1535, 1157	1692[d]

[a] Spectra recorded as Nujol mulls between KBr plates. [b] Catecholate. [c] Hydroxyl. [d] Carboxylate.

Table 2. ^1H NMR Data[a] for Osmium Stannyl Complexes

complex	δ (ppm)
$Os(SnMe_3)(\eta^2\text{-}S_2CNMe_2)(CO)(PPh_3)_2$ (**1**)	−0.46 (s, 9H, $SnCH_3$, $^2J_{SnH}$ = 37.6 Hz), 1.96 (s, 3H, S_2CNMe_2), 2.24 (s, 3H, S_2CNMe_2), 7.20−7.75 (m, 30H, PPh_3)
$Os(SnMe_2I)(\eta^2\text{-}S_2CNMe_2)(CO)(PPh_3)_2$ (**2**)	0.47 (s, 6H, $SnCH_3$, $^2J_{SnH}$ = 32.9 Hz), 1.99 (s, 3H, S_2CNMe_2), 2.23 (s, 3H, S_2CNMe_2), 7.25−7.70 (m, 30H, PPh_3)
$Os(SnMeI_2)(\eta^2\text{-}S_2CNMe_2)(CO)(PPh_3)_2$ (**3**)	1.06 (s, 3H, $SnCH_3$, $^2J_{SnH}$ = 25.6 Hz), 2.00 (s, 3H, S_2CNMe_2), 2.22 (s, 3H, S_2CNMe_2), 7.25−7.70 (m, 30H, PPh_3)
$Os(SnI_3)(\eta^2\text{-}S_2CNMe_2)(CO)(PPh_3)_2$ (**4**)	2.03 (s, 3H, S_2CNMe_2), 2.22 (s, 3H, S_2CNMe_2), 7.25−7.75 (m, 30H, PPh_3)
$Os(SnMeBr_2)(\eta^2\text{-}S_2CNMe_2)(CO)(PPh_3)_2$ (**5**)	0.80 (s, 3H, $SnCH_3$, $^2J_{SnH}$ = 27.9 Hz), 1.98 (s, 3H, S_2CNMe_2), 2.25 (s, 3H, S_2CNMe_2), 7.25−7.97 (m, 30H, PPh_3)
$Os(SnMe[\eta^2\text{-}O_2C_6H_4])(\eta^2\text{-}S_2CNMe_2)(CO)(PPh_3)_2$ (**6**)	0.15 (s, 3H, $SnCH_3$, $^2J_{SnH}$ = 33.5 Hz), 1.78 (s, 3H, S_2CNMe_2), 2.36 (s, 3H, S_2CNMe_2), 6.43 (dd, 2H, cat, $^3J_{HH}$ = 5.6 Hz, $^4J_{HH}$ = 3.6 Hz), 6.61 (dd, 2H, cat, $^3J_{HH}$ = 5.6 Hz, $^4J_{HH}$ = 3.6 Hz), 7.25−7.95 (m, 30H, PPh_3)
$Os(SnMe[SCH_2CH_2S])(\eta^2\text{-}S_2CNMe_2)(CO)(PPh_3)_2$ (**7**)	0.65 (s, 3H, $SnCH_3$, $^2J_{SnH}$ = 32.9 Hz), 1.97 (s, 3H, S_2CNMe_2), 2.23 (s,3H, S_2CNMe_2), 2.71 (s, 4H, SCH_2, $^3J_{SnH}$ = 23.6 Hz), 7.25−7.75 (m, 30H, PPh_3)
$Os(Sn[OH]_3)(\eta^2\text{-}S_2CNMe_2)(CO)(PPh_3)_2$ (**8**)	0.29 br (s, 3H, $SnOH$, $^2J_{SnH}$ = 21.6 Hz), 1.96 (s, 3H, S_2CNMe_2), 2.34 (s, 3H, S_2CNMe_2), 7.25−7.75 (m, 30H, PPh_3)
$Os(Sn[OCH_2CH_2]_3N)(\eta^2\text{-}S_2CNMe_2)(CO)(PPh_3)_2$ (**9**)	1.89 (s, 3H, S_2CNMe_2), 2.23 (t, 6H, $Sn(OCH_2CH_2)_3N$, $^3J_{HH}$ = 5.3 Hz, $^2J_{SnH}$ = 37.7 Hz), 2.31 (s, 3H, S_2CNMe_2), 3.28 (t, 6H, $Sn(OCH_2CH_2)_3N$, $^3J_{HH}$ = 5.3 Hz, $^3J_{SnH}$ = 33.7 Hz), 7.25−7.95 (m, 30H, PPh_3)
$Os(Sn\ [OC(O)CH_2]_3N)(\eta^2\text{-}S_2CNMe_2)(CO)(PPh_3)_2$ (**10**)	1.96 (s, 3H, S_2CNMe_2), 2.35 (s, 3H, S_2CNMe_2), 2.90 (s, 6H, $Sn(OC(O)CH_2)_3N$, $^4J_{SnH}$ = 26.6 Hz), 7.25−7.85 (m, 30H, PPh_3)

[a] Spectra recorded in $CDCl_3$ at 25 °C. Chemical shifts are referenced to Me_4Si (δ = 0.00). Splitting patterns and line shapes are as follows: s = singlet, dd = doublet of doublets, t = triplet, br = broad. Coupling constants involving tin measured from observed satellites, coupling to $^{119}Sn/^{117}Sn$ not resolved.

with a substrate containing two appropriately linked nucleophilic sites, thereby forming a stannacyclic ring. Accordingly, compound **3** reacts with catechol in the presence of triethylamine to give $Os(SnMe[O_2C_6H_4])(\eta^2\text{-}S_2CNMe_2)(CO)(PPh_3)_2$ (**6**) in high yield. In the ^1H NMR spectrum the tin methyl resonance is observed at 0.15 ppm. The catechol protons are observed as two doublets (at 6.43 and 6.61 ppm), and in the ^{13}C NMR spectrum only three signals are observed for the carbon atoms of this ligand (at 114.1, 116.3, and 155.3 ppm), thus confirming the symmetrical nature of the product.

In a similar fashion, **3** reacts with 1,2-ethanedithiol and triethylamine to give $Os(SnMe[SCH_2CH_2S])(\eta^2\text{-}S_2CNMe_2)(CO)(PPh_3)_2$ (**7**). As with **6,** the formation of a five-membered stannacyclic ring in this product is supported by the spectroscopic data (Tables 1−4). The methyl resonance is at 0.65 ppm in the ^1H NMR spectrum, while the methylene protons of the 1,2-dithioethane group appear as a singlet at 2.71 ppm with accompanying tin satellites. Similarly, the ^{13}C NMR spectrum reveals only one carbon signal for the ligand, thus confirming the two carbon atoms as equivalent. An X-ray crystal structure determination has confirmed the nature of this product (see below).

Treatment of compound **3** with pyridinium tribromide ($pyHBr_3$) gives $Os(SnMeBr_2)(\eta^2\text{-}S_2CNMe_2)(CO)(PPh_3)_2$ (**5**). Compound **5** is a white solid and has spectroscopic properties similar to **3**. The structure of **5** has been determined by X-ray crystallography (see below).

Reactions at Tin of $Os(SnI_3)(\eta^2\text{-}S_2CNMe_2)(CO)(PPh_3)_2$ (4) (see Scheme 4). Treatment of **4** with a large excess of aqueous KOH affords the trihydroxystannyl complex $Os(Sn[OH]_3)(\eta^2\text{-}S_2CNMe_2)(CO)(PPh_3)_2$ (**8**). The OH protons, which are seen in the ^1H NMR spectrum as a singlet at 0.29 ppm (with tin satellites), undergo rapid exchange with D_2O. This singlet signal integrates for three protons versus the signals from the dimethyldithiocarbamate ligand, thus supporting the monomeric formulation with a discrete $Sn(OH)_3$ ligand rather than any formulations involving condensed species.

Compound **4** reacts with triethanolamine to give the metal-bound stannatrane $Os(Sn[OCH_2CH_2]_3N)(\eta^2\text{-}S_2CNMe_2)(CO)(PPh_3)_2$ (**9**), which we have previously described, complete with an X-ray crystal structure determination, in a preliminary communication.[6] In a related reaction, treatment of **4** with nitrilotriacetic acid in the presence of triethylamine gives the unusual, metal-bound stannatranone $Os(Sn[OC(O)CH_2]_3N)(\eta^2\text{-}S_2CNMe_2)(CO)(PPh_3)_2$ (**10**). The crystal structure of **10** has been determined (see below). A single resonance is observed for the six equivalent methylene protons at 2.90 ppm (with tin satellites).

Table 3. ^{13}C NMR Data[a] for Selected Osmium Stannyl Complexes

complex	δ (ppm)
Os(SnMe[η^2-$O_2C_6H_4$])(η^2-S_2CNMe_2)(CO)(PPh_3)$_2$ (**6**)[b]	7.41 (Sn*Me*, $^2J_{SnC}$ = 122.6 Hz), 36.18 (S_2CN*Me*$_2$), 36.33 (S_2CN*Me*$_2$), 114.07 (cat), 116.30 (cat), 127.66 (t′[c], $^{2,4}J_{CP}$ = 10 Hz, *o*-PPh_3), 129.74 (*p*-PPh_3), 134.56 (t′, $^{3,5}J_{CP}$=10 Hz, *m*-PPh_3), 135.40 (t′, $^{1,3}J_{CP}$ = 50 Hz, *i*-PPh_3), 155.3 (cat), 209.45 (S_2*C*NMe_2)
Os(SnMe[SCH_2CH_2S])(η^2-S_2CNMe_2)(CO)(PPh_3)$_2$ (**7**)	4.58 (Sn*Me*, $^2J_{SnC}$ = 120.2 Hz), 36.11 (S_2CN*Me*$_2$), 36.33 (S_2CN*Me*$_2$), 36.77 (*S*CH_2, ^2J(SnC) = 25.1 Hz), 127.23 (t′, $^{2,4}J_{CP}$ = 10 Hz, *o*-PPh_3), 129.55 (*p*-PPh_3), 133.90 (t′, $^{1,3}J_{CP}$ = 48 Hz, *i*-PPh_3), 134.97 (t′, $^{3,5}J_{CP}$ = 10 Hz, *m*-PPh_3), 185.90 (t, $^2J_{PC}$ = 19.3 Hz, *C*O), 208.95 (S_2*C*NMe_2)
Os(Sn[$OCH_2CH_2]_3N$)(η^2-S_2CNMe_2)(CO)(PPh_3)$_2$ (**9**)	35.80 (S_2CN*Me*$_2$), 36.42 (S_2CN*Me*$_2$), 53.30 (Sn(O*C*$H_2CH_2)_3N$, $^2J_{SnC}$ = 34.2 Hz), 57.39 (Sn(O*C*$H_2CH_2)_3N$, $^2J_{SnC}$ = 42.4 Hz), 126.76 (t′, $^{2,4}J_{CP}$ = 11 Hz, *o*-PPh_3), 128.67 (*p*-PPh_3), 129.78 (t′, $^{1,3}J_{CP}$ = 52 Hz, *i*-PPh_3), 135.27 (t′, $^{3,5}J_{CP}$ = 10 Hz, *m*-PPh_3), 185.61 (t, $^2J_{PC}$ = 18.5 Hz, *C*O), 210.59 (S_2*C*NMe_2)
Os(Sn [OC(O)$CH_2]_3N$)(η^2-S_2CNMe_2)(CO)(PPh_3)$_2$ (**10**)	36.22 (S_2CN*Me*$_2$), 58.29 (Sn(OC(O)*C*$H_2)_3N$, $^3J_{SnC}$ = 36.2 Hz), 127.68 (t′, $^{2,4}J_{CP}$ = 10 Hz, *o*-PPh_3), 129.98 (*p*-PPh_3), 134.10 (t′, $^{1,3}J_{CP}$ = 52 Hz, *i*-PPh_3), 134.88 (t′, $^{3,5}J_{CP}$ = 10 Hz, *m*-PPh_3), 168.96 (Sn(O*C*(O)$CH_2)_3N$, $^2J_{SnC}$ = 36.2 Hz), 181.40 (t, $^2J_{PC}$ = 18.5 Hz, *C*O), 208.48 (S_2*C*NMe_2)

[a] Spectra recorded in $CDCl_3$ at 25 °C. Chemical shifts are referenced to $CDCl_3$ (δ = 77.00). Coupling constants involving tin measured from observed satellites, coupling to ^{119}Sn/^{117}Sn not resolved. [b] Signal for CO ligand not observed due to low solubility. [c] t′ denotes that the signal has apparent triplet multiplicity; $^{n,m}J$(C,P) is the sum of the two coupling constants ^mJ(C,P) and ^nJ(C,P) as explained in: Maddock, S. M.; Rickard, C. E. F.; Roper, W. R.; Wright, L. J. *Organometallics* **1996**, *15*, 1793−1803.

Table 4. ^{119}Sn NMR Data for Selected Osmium Stannyl Complexes

complex	δ (ppm)
Os($SnMe_3$)(η^2-S_2CNMe_2)(CO)(PPh_3)$_2$ (**1**)[a]	−176.8 (t, $^2J_{SnP}$ = 89.52 Hz)
Os($SnMeI_2$)(η^2-S_2CNMe_2)(CO)(PPh_3)$_2$ (**3**)[a]	−205.7 (t, $^2J_{SnP}$ = 89.52 Hz)
Os(SnI_3)(η^2-S_2CNMe_2)(CO)(PPh_3)$_2$ (**4**)[b]	−746.8 (t, $^2J_{SnP}$ = 82.01 Hz)
Os(SnMe[η^2-$O_2C_6H_4$])(η^2-S_2CNMe_2)(CO)(PPh_3)$_2$ (**6**)[a]	74.85 (t, $^2J_{SnP}$ = 125.89 Hz)
Os(SnMe[SCH_2CH_2S])(η^2-S_2CNMe_2)(CO)(PPh_3)$_2$ (**7**)[a]	0.12 (t, $^2J_{SnP}$ = 103.70 Hz)
Os(Sn[OH]$_3$)(η^2-S_2CNMe_2)(CO)(PPh_3)$_2$ (**8**)[a]	−370.6 (t, $^2J_{SnP}$ = 164.09 Hz)
Os(Sn[$OCH_2CH_2]_3N$)(η^2-S_2CNMe_2)(CO)(PPh_3)$_2$ (**9**)[a]	−513.4 (t, $^2J_{SnP}$ = 193.86 Hz)
Os(Sn[OC(O)$CH_2]_3N$)(η^2-S_2CNMe_2)(CO)(PPh_3)$_2$ (**10**)[a]	−778.1 (t, $^2J_{SnP}$ = 178.90 Hz)

[a] Spectra recorded in $CDCl_3$−$CHCl_3$ (1:3) at 25 °C. Chemical shifts are referenced to $SnMe_4$ (δ = 0.00). [b] Recorded in CD_2Cl_2−CH_2Cl_2 (1:3)

^{119}Sn NMR Studies. For each of the compounds studied, the tin atom was observed in the ^{119}Sn NMR-{^{1}H} spectrum as a triplet signal, through coupling to the two mutually *trans* triphenylphosphine ligands. The tin chemical shift moves to higher field as methyl groups are replaced by iodide in the compounds Os($SnMe_3$)(η^2-S_2CNMe_2)(CO)(PPh_3)$_2$ (**1**) (δ = −176.8 ppm), Os($SnMeI_2$)(η^2-S_2CNMe_2)(CO)(PPh_3)$_2$ (**3**) (δ = −205.7 ppm), and Os(SnI_3)(η^2-S_2CNMe_2)(CO)(PPh_3)$_2$ (**4**) (δ = −746.8 ppm). For comparison, SnI_4 has a chemical shift of −1701 ppm.[11] In Os(Sn[$OCH_2CH_2]_3N$)(η^2-S_2CNMe_2)(CO)(PPh_3)$_2$ (**9**) the tin signal is seen at −513.4 ppm. The tin signal for Os(Sn[OC(O)$CH_2]_3N$)(η^2-S_2CNMe_2)(CO)(PPh_3)$_2$ (**10**) is found at even higher field, at −778.1 ppm. Other examples for stannatrane systems are $Me_2N(CH_2)_3Sn(OCH_2CH_2)_3N$ (−291.2 ppm)[12] and ^{n}BuSn($OCH_2CH_2)_3N$ (−246 ppm for a five-coordinate site and −383 ppm for a six-coordinate site).[13]

Crystallographic Studies. X-ray crystal structures were determined for complexes **1**, **4**, **5**, **7**, and **10**. The structure of complex **9** has already been described.[6] Crystal and refinement data are given in Table 5, and selected bond lengths (Å) and angles appear in Tables 6−10.

The molecular structures of **1**, **4**, **5**, **7**, and **10** are depicted in Figures 1−5, respectively. The overall geometry at the osmium center is the same for all the structures presented here and can best be described as distorted octahedral with the two triphenylphosphine ligands mutually *trans*, and with the η^2-bonded dithiocarbamate, the stannyl ligand, and the carbon monoxide in the equatorial plane. The two triphenylphosphine ligands in each of the compounds adopt an eclipsed arrangement, and as can be seen in Figures 1−5, even the relative orientations of the phenyl rings are almost identical. Because of this constancy of the accompanying ligand environment, the major feature of interest in these structures lies with the structural parameters associated with the coordination geometry of the tin atom. In each structure one of the three substituents bound to tin is found lying approximately in the equatorial plane of the complex defined by Os, S(1), S(2), C(1), and Sn. The following discussion considers each structure in turn and focuses most attention on the Os−SnR_3 moiety.

In the structure of Os($SnMe_3$)(η^2-S_2CNMe_2)(CO)(PPh_3)$_2$ (see Figure 1), angular distortions away from tetrahedral geometry at tin are apparent, with the three Os−Sn−C angles being 110.47(12)°, 117.5(2)°, and 120.93(14)°. The largest angle is associated with the methyl group (C(7)) which is lying in the equatorial plane. Previously reported Os−$SnMe_3$ structures also show angles slightly larger than tetrahedral, e.g., for $HOs_3(\mu_3$-S)(μ_3-$SCH_2)(CO)_{10}(SnMe_3)(PMe_2Ph)$,[14] 111.1-(4)°, 113.4(4)°, 112.0(3)°, and for $Os_3(\mu$-H)$_2(CO)_{10}$-$(SnMe_3)_2$,[15] 108(2)°, 111(2)°, 117(2)° and 109(2)°, 112(1)°,

(11) Burke, J. J.; Lauterbur, P. C. *J. Am. Chem. Soc.* **1961**, *83*, 326.
(12) Dakternieks, D.; Dyson, G.; Jurkschat, K.; Tozer, R.; Tiekink, E. R. T. *J. Organomet. Chem.* **1993**, *458*, 29.
(13) Jurkschat, K.; Mügge, C.; Tzschach, A.; Zschunke, A.; Fischer, G. W. *Z. Anorg. Allg. Chem.* **1980**, *463*, 123.
(14) Adams, R. D.; Katahira, D. A. *Organometallics* **1982**, *1*, 460.

Table 5. Crystal and Refinement Data for 1, 4, 5, 7, and 10

	1	4	5	7	10
empirical formula	$C_{43}H_{45}NOOsP_2S_2Sn$	$C_{40}H_{36}I_3NOOsP_2S_2Sn$	$C_{41}H_{39}Br_2NOOsP_2S_2Sn{\cdot}CH_2Cl_2$	$C_{43}H_{43}NOOsP_2S_4Sn{\cdot}CH_2Cl_2{\cdot}EtOH$	$C_{46}H_{42}N_2O_7OsP_2S_2Sn{\cdot}1.5CH_2Cl_2{\cdot}2H_2O$
fw	1026.75	1362.35	1241.43	1219.85	1333.19
temp, K	193(2)	203(2)	203(2)	203(2)	203(2)
wavelength, Å	0.71073	0.71073	0.71073	0.71073	0.71073
cryst syst	triclinic	monoclinic	monoclinic	triclinic	monoclinic
space group	$P\bar{1}$	$P2_1/n$	$P2_1/n$	$P\bar{1}$	$P2_1/n$
a, Å	11.4006(14)	10.3132(4)	15.5031(2)	12.43020(10)	12.6107(3)
b, Å	12.567(2)	22.2136(7)	15.1872(2)	12.8996(2)	18.9435(5)
c, Å	16.035(8)	19.0702(7)	19.81140(10)	16.4052(2)	23.7628(7)
α, deg	67.10(2)	90	90	95.15	90
β, deg	77.22(2)	91.5190(10)	99.5160(10)	103.99	101.97
γ, deg	79.435(11)	90	90	104.81	90
volume, Å^3	2051.7(11)	4367.3(3)	4600.38(9)	2435.23(5)	5553.3(3)
Z	2	4	4	2	4
density (calc), g cm^{-3}	1.662	2.072	1.789	1.664	1.590
abs coeff, mm^{-1}	3.916	5.799	5.348	3.504	3.064
F(000)	1012	2552	2392	1208	2620
cryst size, mm	0.40 × 0.32 × 0.25	0.20 × 0.08 × 0.05	0.47 × 0.31 × 0.13	0.45 × 0.24 × 0.10	0.50 × 0.09 × 0.07
θ range for data collection	1.40−25.96	1.83−26.38	1.55−26.36	1.65−27.57	1.39−27.61
index ranges	$-13 \le h \le 12$ $-14 \le k \le 13$ $-19 \le l \le 0$	$-12 \le h \le 12$ $0 \le k \le 27$ $0 \le l \le 23$	$-19 \le h \le 19$ $0 \le k \le 18$ $0 \le l \le 24$	$-16 \le h \le 15$ $-16 \le k \le 16$ $0 \le l \le 21$	$-16 \le h \le 15$ $0 \le k \le 24$ $0 \le l \le 30$
no. of reflns collected	7271	24 867	25 078	24 443	33 799
no. of reflns obsd [$I > 2\sigma(I)$]	6284	4918	7718	9836	10 142
indep reflns	7005 [R(int) = 0.0214]	8802 [R(int) = 0.1072]	9328 [R(int) = 0.0314]	10 678 [R(int) = 0.0288]	12 182 [R(int) = 0.00448]
max. and min. transmission	0.4410 and 0.3034	0.7603 and 0.3901	0.5431 and 0.1877	0.7208 and 0.3016	0.8141 and 0.3096
no. of data/restraints/params	7005/0/500	8802/0/462	9328/0/484	10678/0/535	12182/12/611
final R indices [$I > 2\sigma(I)$]	R1 = 0.0257, wR2 = 0.0634	R1 = 0.0623, wR2 = 0.0929	R1 = 0.0311, wR2 = 0.0732	R1 = 0.0287, wR2 = 0.0753	R1 = 0.0475, wR2 = 0.1316
R indices (all data)	R1 = 0.0327, wR2 = 0.0661	R1 = 0.1447, wR2 = 0.1162	R1 = 0.0437, wR2 = 0.0788	R1 = 0.0323, wR2 = 0.0777	R1 = 0.0621, wR2 = 0.1399
goodness-of-fit on F^2	1.028	0.999	1.043	1.039	1.012
largest diff peak and hole, e Å^{-3}	1.254 and −1.326	1.673 and −1.170	1.720 and −1.549	1.807 and −1.391	2.277 and −1.163

Table 6. Selected Bond Distances (Å) and Angles (deg) for Complex 1

Interatomic Distances			
Os−Sn	2.6616(13)	Os−P(2)	2.3879(11)
Os−P(1)	2.3632(11)	Os−C(1)	1.838(4)
Os−S(1)	2.4906(13)	Os−S(2)	2.4656(13)
Sn−C(5)	2.189(4)	Sn−C(6)	2.188(5)
Sn−C(7)	2.168(5)		
Interatomic Angles			
Sn−Os−C(1)	90.01(14)	Sn−Os−S(1)	155.09(3)
Sn−Os−S(2)	84.35(4)	Sn−Os−P(2)	97.42(4)
Sn−Os−P(1)	95.43(4)	C(1)−Os−S(1)	114.87(14)
C(1)−Os−S(2)	174.36(14)	C(1)−Os−P(2)	89.63(13)
C(1)−Os−P(1)	89.57(13)	P(2)−Os−S(1)	84.68(4)
P(2)−Os−S(2)	91.20(4)	P(2)−Os−P(1)	167.13(4)
S(1)−Os−S(2)	70.77(4)	S(1)−Os−P(1)	84.01(4)
S(2)−Os−P(1)	90.86(4)	Os−Sn−C(5)	110.47(12)
Os−Sn−C(6)	117.5(2)	Os−Sn−C(7)	120.93(14)
C(7)−Sn−C(5)	105.4(2)	C(7)−Sn−C(6)	101.5(2)
C(5)−Sn−C(6)	98.13(19)		

Table 7. Selected Bond Distances (Å) and Angles (deg) for Complex 4

Interatomic Distances			
Os−Sn	2.6260(9)	Os−P(2)	2.414(3)
Os−P(1)	2.395(3)	Os−C(1)	1.842(13)
Os−S(1)	2.454(3)	Os−S(2)	2.457(3)
Sn−I(1)	2.7598(12)	Sn−I(2)	2.7688(11)
Sn−I(3)	2.7602(11)		
Interatomic Angles			
Sn−Os−C(1)	94.1(3)	Sn−Os−S(1)	157.41(8)
Sn−Os−S(2)	86.21(7)	Sn−Os−P(2)	98.08(8)
Sn−Os−P(1)	96.62(8)	C(1)−Os−S(1)	108.5(4)
C(1)−Os−S(2)	178.2(4)	C(1)−Os−P(2)	87.3(4)
C(1)−Os−P(1)	88.9(4)	P(2)−Os−S(1)	83.34(10)
P(2)−Os−S(2)	90.96(11)	P(2)−Os−P(1)	165.05(10)
S(1)−Os−S(2)	71.22(10)	S(1)−Os−P(1)	83.34(10)
S(2)−Os−P(1)	92.74(11)	Os−Sn−I(1)	111.53(3)
Os−Sn−I(2)	126.73(4)	Os−Sn−I(3)	120.71(4)
I(1)−Sn−I(2)	102.08(4)	I(1)−Sn−I(3)	94.67(4)
I(2)−Sn−I(3)	95.30(3)		

Table 8. Selected Bond Distances (Å) and Angles (deg) for Complex 5

Interatomic Distances			
Os−Sn	2.6065(3)	Os−P(2)	2.3886(11)
Os−P(1)	2.3937(11)	Os−C(1)	1.863(5)
Os−S(1)	2.4685(10)	Os−S(2)	2.4537(11)
Sn−C(5)	2.165(5)	Sn−Br(2)	2.5680(6)
Sn−Br(1)	2.5899(6)		
Interatomic Angles			
Sn−Os−C(1)	92.02(13)	Sn−Os−S(1)	158.69(3)
Sn−Os−S(2)	87.77(3)	Sn−Os−P(2)	95.44(3)
Sn−Os−P(1)	96.92(3)	C(1)−Os−S(1)	109.29(13)
C(1)−Os−S(2)	178.56(14)	C(1)−Os−P(2)	87.75(14)
C(1)−Os−P(1)	88.12(14)	P(2)−Os−S(1)	85.73(4)
P(2)−Os−S(2)	93.68(4)	P(2)−Os−P(1)	167.10(4)
S(1)−Os−S(2)	70.92(4)	S(1)−Os−P(1)	84.11(4)
S(2)−Os−P(1)	90.50(4)	Os−Sn−C(5)	134.70(14)
Os−Sn−Br(2)	111.344(17)	Os−Sn−Br(1)	113.084(17)
C(5)−Sn−Br(2)	99.24(15)	C(5)−Sn−Br(1)	97.82(15)
Br(2)−Sn−Br(1)	92.01(2)		

113(2)°. Any explanation of these observations must include consideration of both steric and electronic effects. The Os−Sn bond distance is 2.6616(13) Å. For comparison we note that the Os−Sn distance in $HOs_3(\mu_3\text{-}S)(\mu_3\text{-}SCH_2)(CO)_{10}(SnMe_3)(PMe_2Ph)$[14] is 2.653(1) Å, and for the two distances in $Os_3(\mu\text{-}H)_2(CO)_{10}(SnMe_3)_2$-15 the values are 2.726(5) and 2.696(4) Å.

(15) Einstein, F. W. B.; Pomeroy, R. K.; Willis, A. C. *J. Organomet. Chem.* **1986**, *311*, 257.

Table 9. Selected Bond Distances (Å) and Angles (deg) for Complex 7

Interatomic Distances			
Os−Sn	2.6329(2)	Os−P(2)	2.3687(8)
Os−P(1)	2.3746(8)	Os−C(1)	1.855(4)
Os−S(1)	2.4780(9)	Os−S(2)	2.4579(9)
Sn−C(7)	2.165(4)	Sn−S(3)	2.4890(11)
Sn−S(4)	2.4571(9)	S(3)−C(5)	1.830(5)
C(5)−C(6)	1.811(4)	C(6)−S(4)	1.811(4)
Interatomic Angles			
Sn−Os−C(1)	93.48(11)	Sn−Os−S(1)	158.50(2)
Sn−Os−S(2)	87.84(2)	Sn−Os−P(2)	92.24(2)
Sn−Os−P(1)	93.20(2)	C(1)−Os−S(1)	108.01(11)
C(1)−Os−S(2)	178.65(11)	C(1)−Os−P(2)	88.08(11)
C(1)−Os−P(1)	87.40(11)	P(2)−Os−S(1)	89.06(3)
P(2)−Os−S(2)	92.13(3)	P(2)−Os−P(1)	173.13(3)
S(1)−Os−S(2)	70.66(3)	S(1)−Os−P(1)	87.42(3)
S(2)−Os−P(1)	92.27(3)	Os−Sn−C(7)	129.61(11)
Os−Sn−S(3)	115.45(3)	Os−Sn−S(4)	113.50(2)
C(7)−Sn−S(3)	100.03(13)	C(7)−Sn−S(4)	101.61(13)
S(3)−Sn−S(4)	88.20(3)		

Table 10. Selected Bond Distances (Å) and Angles (deg) for Complex 10

Interatomic Distances			
Os−Sn	2.5901(4)	Os−P(1)	2.4041(15)
Os−P(2)	2.3929(15)	Os−C(1)	1.875(6)
Os−S(1)	2.4542(15)	Os−S(2)	2.4653(16)
Sn−O(2)	2.134(5)	Sn−O(3)	2.087(5)
Sn−O(4)	2.109(5)	Sn−N(2)	2.357(5)
N(2)−C(10)	1.478(13)	N(2)−C(8)	1.40(3)
N(2)−C(8′)	1.503(15)	N(2)−C(6)	1.446(12)
O(4)−C(9)	1.283(9)	O(7)−C(9)	1.213(11)
C(10)−C(9)	1.508(15)	O(2)−C(5)	1.281(9)
O(5)−C(5)	1.222(11)	C(6)−C(5)	1.537(15)
O(3)−C(7)	1.282(9)	O(6)−C(7)	1.215(9)
C(8)−C(7)	1.49(3)	C(8′)−C(7)	1.569(15)
Interatomic Angles			
Sn−Os−C(1)	94.28(18)	Sn−Os−S(1)	159.83(4)
Sn−Os−S(2)	88.71(4)	Sn−Os−P(1)	93.04(4)
Sn−Os−P(2)	94.17(4)	C(1)−Os−S(1)	105.87(19)
C(1)−Os−S(2)	176.88(19)	C(1)−Os−P(1)	88.56(18)
C(1)−Os−P(2)	89.26(18)	P(1)−Os−S(1)	86.99(5)
P(1)−Os−S(2)	90.39(5)	P(1)−Os−P(1)	172.60(5)
S(1)−Os−S(2)	71.12(5)	S(1)−Os−P(2)	86.81(5)
S(2)−Os−P(2)	91.42(5)	Os−Sn−O(2)	107.57(14)
Os−Sn−O(3)	111.90(13)	Os−Sn−O(4)	101.96(15)
O(2)−Sn−O(3)	110.1(2)	O(4)−Sn−O(2)	122.7(2)
O(3)−Sn−O(4)	102.3(2)	O(4)−Sn−N(2)	73.5(2)
O(3)−Sn−N(2)	73.8(2)	O(2)−Sn−N(2)	72.1(2)
Sn−N(2)−C(10)	108.1(6)	Sn−N(2)−C(8)	109.0(13)
Sn−N(2)−C(8′)	103.8(6)	Sn−N(2)−C(6)	107.5(5)
C(10)−N(2)−C(8)	90.0(15)	C(10)−N(2)−C(8′)	115.6(9)
C(10)−N(2)−C(6)	113.4(9)	C(6)−N(2)−C(8)	127.0(16)
C(6)−N(2)−C(8′)	107.8(9)	C(8)−N(2)−C(8′)	26.2(14)

The molecular structure of $Os(SnI_3)(\eta^2\text{-}S_2CNMe_2)(CO)(PPh_3)_2$ is shown in Figure 2. The arrangement of the three iodide substituents about tin is the same as that for the three methyl groups about tin in the structure of **1**, in that one iodide lies in the equatorial plane. The distortion away from idealized tetrahedral is now even more pronounced; the Os−Sn−I bonding angles are 111.53(3)°, 120.71(4)°, and 126.73(4)°. Again, the largest angle is associated with the iodide (I(2)) lying in the equatorial plane. The osmium−tin bond distance is 2.6460(9) Å. The greater inductive effect exerted by the more electronegative iodine atoms as opposed to the methyl groups may be a factor in explaining the slight reduction in Os−Sn distance compared with **1**.

The molecular structure of $Os(SnMeBr_2)(\eta^2\text{-}S_2CNMe_2)(CO)(PPh_3)_2$ is depicted in Figure 3. The single methyl

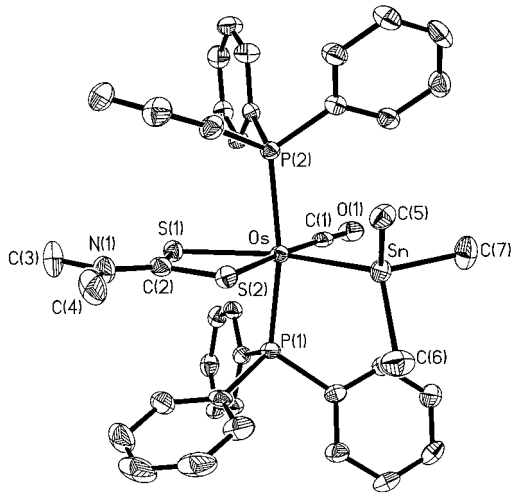

Figure 1. Molecular structure of $Os(SnMe_3)(\eta^2\text{-}S_2CNMe_2)(CO)(PPh_3)_2$ (**1**) with thermal ellipsoids at the 50% probability level.

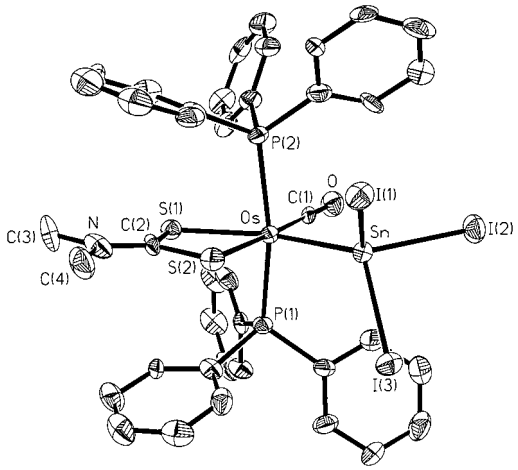

Figure 2. Molecular structure of $Os(SnI_3)(\eta^2\text{-}S_2CNMe_2)(CO)(PPh_3)_2$ (**4**) with thermal ellipsoids at the 50% probability level.

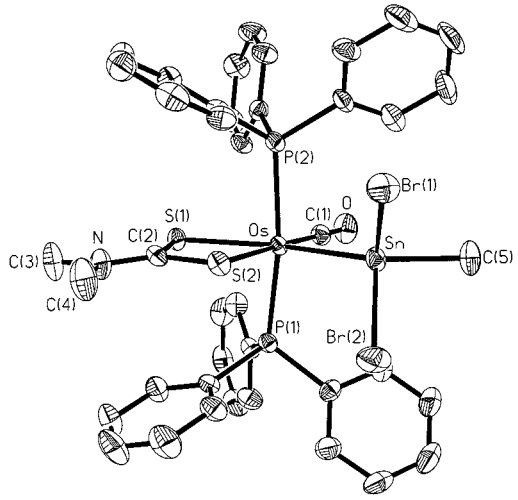

Figure 3. Molecular structure of $Os(SnMeBr_2)(\eta^2\text{-}S_2CNMe_2)(CO)(PPh_3)_2$ (**5**) with thermal ellipsoids at the 50% probability level.

group is found lying in the equatorial plane. The angular distortions at the tin center of the dihaloorganostannyl moiety are similar to those observed in previous structure determinations of $SnRX_2$ complexes.[16] The Os−Sn−C angle is very large at 134.70(14)°, while the Os−Sn−Br angles are 111.344(17)° and 113.084(17)°. The greater electronegativity of bromide over iodide contributes to an even shorter Os−Sn bond distance than for the triiodostannyl complex, with Os−Sn at 2.6065(3) Å.

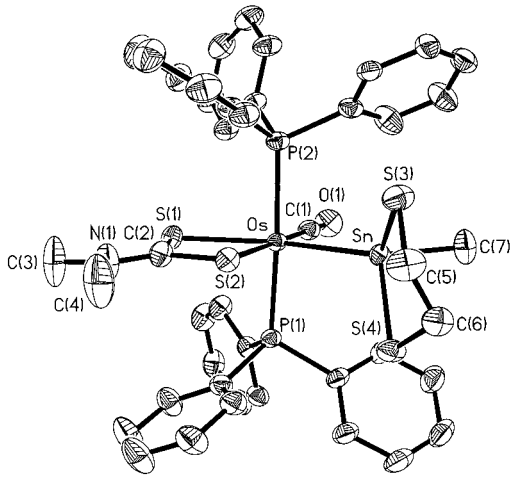

Figure 4. Molecular structure of $Os(SnMe[1,2\text{-}S_2C_2H_4])(\eta^2\text{-}S_2CNMe_2)(CO)(PPh_3)_2$ (**7**) with thermal ellipsoids at the 50% probability level.

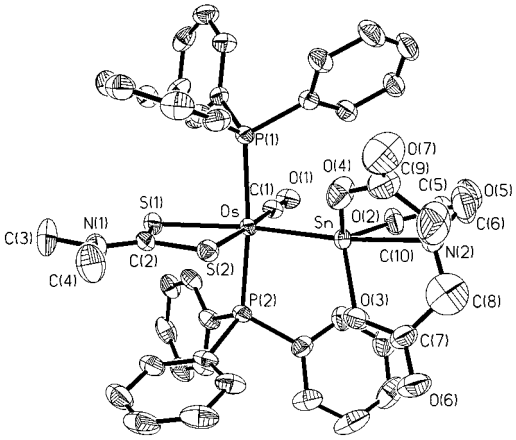

Figure 5. Molecular structure of $Os(Sn[OC(O)CH_2]_3N)(\eta^2\text{-}S_2CNMe_2)(CO)(PPh_3)_2$ (**10**) with thermal ellipsoids at the 50% probability level.

The molecular structure of $Os(SnMe[1,2\text{-}S_2C_2H_4])(\eta^2\text{-}S_2CNMe_2)(CO)(PPh_3)_2$ is depicted in Figure 4. The geometry at the tin center closely resembles that found in complex **5**, with the positions of the bromide ligands taken by sulfur atoms from the dithiol ligand. Again the carbon atom from the tin-methyl group lies in the equatorial plane. The Os−Sn−C angle, at 129.61(11)°, is significantly larger than the two Os−Sn−S angles, which are 113.50(2)° and 115.45(3)°. The "bite angle" of the dithiol ligand is only 88.20(3)°, with the angles in the metallocyclic ring all normal. There is very little difference in the C−Sn−S angles, at 101.61(13)° and 100.03(13)°. The two Sn−S bond distances, 2.4571(9) and 2.4890(11) Å, are similar to that found in $Ru(SnMe_2$-

(16) (a) Sasse, H. E.; Ziegler, M. L. *Z. Anorg. Allg. Chem.* **1973**, *402*, 129. (b) Greene, P. T.; Bryan, R. F. *J. Chem. Soc. (A)* **1970**, 2261. (c) Elder, M.; Graham, W. A. G.; Hall, D.; Kummer, R. *J. Am. Chem. Soc.* **1968**, *90*, 2189. (d) Miguel, D.; Pérez-Martínez, J. A.; Riera, V. *Polyhedron* **1991**, *10*, 1717.

SH)I(CO)(CN[*p*-tolyl])(PPh_3)$_2$[5] (2.481(4) Å). The osmium−tin distance, 2.6329(2) Å, is longer than the values for **4** or **5**, but shorter than in **1**.

The molecular structure of Os(Sn[OC(O)CH_2]$_3$N)(η^2-S_2CNMe_2)(CO)(PPh_3)$_2$ is depicted in Figure 5. Carbon atom C(8) is disordered over two sites and was modeled with a 50% occupancy. No other atoms in the molecule are affected. Confirmation of the stannatranone cage structure is the most interesting feature of the structure. The transannular Sn−N(2) distance is 2.356(5) Å. This is longer than that found in the unmetalated stannatranone, Me_2(O)N(CH_2)$_3$Sn(OCOCH_2)$_3$N[12] (2.231(7) Å), but is slightly shorter than the corresponding Sn−N distance (2.422(4) Å) found in the related stannatrane complex Os(Sn[OCH_2CH_2]$_3$N)(η^2-S_2CNMe_2)(CO)(PPh_3)$_2$ (**9**)[6] and clearly must represent a bonding interaction. The geometry at the nitrogen is close to tetrahedral, with the nitrogen facing in toward the tin atom. The Os−Sn bond distance is very short, at 2.5901(4) Å. This is shorter than the corresponding bond in the related stannatrane complex **9** and is presumably a consequence of the more electronegative groups (carboxylate rather than alkoxide) on the tin.

Conclusion. A redistribution reaction between a trimethyltin osmium complex and SnI_4 offers an effective route to a diiodostannyl complex, whereas iodine cleaves not only Sn−Me bonds but also Os−Sn bonds. The redistribution process is even effective between two complexed stannyl ligands. The resulting iodinated ligands are ideal substrates for the introduction of unusual functionalities at tin, and novel stannyl ligands that have been built in situ include [Os]−Sn(OH)$_3$, [Os]−Sn(OCOCH_2)$_3$N, and [Os]−SnMe($S_2C_2H_4$).

Experimental Section

General Considerations. All reactions were carried out using standard Schlenk techniques under nitrogen, but final recrystallizations were carried out in the open. Solvents were dried by standard techniques and distilled under nitrogen before use. Os($SnMe_3$)(Cl)(CO)(PPh_3)$_2$ was prepared from OsHCl(CO)(PPh_3)$_3$ and trimethylvinyltin.[4] All other compounds were commercially obtained and used without further purification.

NMR spectra (^{1}H, ^{13}C, and ^{119}Sn) were recorded on a Bruker DRX 400 NMR spectrometer. IR spectra were recorded as Nujol mulls between KBr plates using a Perkin-Elmer FT-IR Spectrum 1000 spectrometer. Elemental analyses (C, H, N) were carried out at the Microanalytical Laboratory, University of Otago.

Os($SnMe_3$)(η^2-S_2CNMe_2)(CO)(PPh_3)$_2$ (1). A red solution of Os($SnMe_3$)(Cl)(CO)(PPh_3)$_2$[4] produced from OsHCl(CO)(PPh_3)$_3$ (1.00 g, 0.960 mmol) was cooled to 0 °C in an ice bath, and NaS_2CNMe_2·2H_2O (0.172 g, 0.960 mmol) dissolved in methanol (10 mL) was added directly. The red color rapidly changed to pale yellow (ca. 2 s). The reaction was stirred for 30 min and then ethanol (20 mL) added. The solvent volume was reduced in vacuo to 5 mL, and the resulting yellow solid was collected via filtration. This was recrystallized from dichloromethane/ethanol to give pure **1** as a pale yellow solid (0.816 g, 82.8%). Anal. Calcd for $C_{43}H_{45}NOP_2S_2SnOs$: C, 50.30; H, 4.42; N, 1.36. Found: C, 50.71; H, 3.85; N, 1.33.

Os($SnMe_2I$)(η^2-S_2CNMe_2)(CO)(PPh_3)$_2$ (2). To a stirred, orange solution of Os($SnMeI_2$)(η^2-S_2CNMe_2)(CO)(PPh_3)$_2$ (0.081 g, 0.065 mmol) in benzene (20 mL) was added Os($SnMe_3$)(η^2-S_2CNMe_2)(CO)(PPh_3)$_2$ (0.066 g, 0.065 mmol) also in benzene (20 mL). The reaction was heated to 40 °C for 18 h. Total solvent removal in vacuo and recrystallization of the residue from dichloromethane−ethanol gave pure **2** as a tan microcrystalline solid (0.089 g, 60.3%). Anal. Calcd for $C_{42}H_{42}NOP_2S_2SnOsI$: C, 44.30; H, 3.72; N, 1.23. Found: C, 44.63; H, 3.82; N, 1.30.

Os($SnMeI_2$)(η^2-S_2CNMe_2)(CO)(PPh_3)$_2$ (3). To a yellow solution of Os($SnMe_3$)(Cl)(CO)(PPh_3)$_2$ (0.495 g, 0.482 mmol) in benzene (20 mL) was added a solution of SnI_4 (2.505 g, 4.00 mmol) in benzene (40 mL). The initial deep orange-brown solution was stirred at room temperature for 12 h, after which time a small quantity of yellow precipitate had formed. Solvent removal in vacuo gave a brown paste. Two recrystallizations from dichloromethane−ethanol provided pure **3** as a yellow microcrystalline solid (0.414 g, 68.7%). Anal. Calcd for $C_{41}H_{39}NOP_2S_2SnOsI_2$: C, 39.38; H, 3.14; N, 1.12. Found: C, 39.50; H, 3.07; N, 1.31.

Os(SnI_3)(η^2-S_2CNMe_2)(CO)(PPh_3)$_2$ (4). Os($SnMeI_2$)(η^2-S_2CNMe_2)(CO)(PPh_3)$_2$ (0.512 g, 0.409 mmol) was dissolved in dichloromethane (20 mL), and the resulting yellow solution was then chilled to 0 °C. Iodine (0.110 g, 0.433 mmol) in dichloromethane (40 mL) was added dropwise over 1 h, with constant stirring. After complete addition the purple solution was allowed to warm to room temperature and then stirred for a further hour. Addition of ethanol (20 mL) and the removal of solvent in vacuo caused the precipitation of a yellow solid, which was collected via filtration and recrystallized from dichloromethane−ethanol. Pure **4** was obtained as orange microcrystals (0.423 g, 75.9%). Anal. Calcd for $C_{40}H_{36}NOP_2S_2SnOsI_3$: C, 35.26; H, 2.66; N, 1.03. Found: C, 36.02; H, 2.66; N, 1.09.

Os($SnMeBr_2$)(η^2-S_2CNMe_2)(CO)(PPh_3)$_2$ (5). To an orange, stirred solution of Os($SnMeI_2$)(η^2-S_2CNMe_2)(CO)(PPh_3)$_2$ (0.100 g, 0.085 mmol) in benzene (20 mL) was added a solution of pyridinium tribromide (0.035 g, 0.109 mmol) in dichloromethane (10 mL). The reaction was stirred for 14 h, after which time a quantity of white precipitate had formed. This was separated by filtration and recrystallized from dichloromethane−ethanol to give pure **5** as a white microcrystalline solid (0.070 g, 81.2%). Anal. Calcd for $C_{41}H_{39}NOS_2P_2OsSnBr_2$·2$CH_2Cl_2$: C, 38.94; H, 3.27; N, 1.06. Found: C, 38.86; H, 3.19; N, 1.23.

Os(SnMe[η^2-$O_2C_6H_4$])(η^2-S_2CNMe_2)(CO)(PPh_3)$_2$ (6). To a yellow, stirred solution of Os($SnMeI_2$)(η^2-S_2CNMe_2)(CO)(PPh_3)$_2$ (0.096 g, 0.077 mmol) in dichloromethane (30 mL) was added a solution of catechol (0.040 g, 0.363 mmol) in dichloromethane (10 mL). No visual change was apparent. Addition of triethylamine (0.5 mL) caused the color to fade rapidly over about 5 s. The resulting colorless solution was stirred at room temperature for 1 h. The organic layer was washed with water (3 × 20 mL) and then filtered. Addition of ethanol (20 mL) and solvent reduction in vacuo to 5 mL provided pure **6** as a white microcrystalline solid (0.056 g, 65.9%). Anal. Calcd for $C_{47}H_{43}NO_3P_2S_2OsSn$·1/3$CH_2Cl_2$: C, 50.17; H, 3.88; N, 1.24. Found: C, 50.22; H, 4.03; N, 1.31.

Os(SnMe[SCH_2CH_2S])(η^2-S_2CNMe_2)(CO)(PPh_3)$_2$ (7). To a yellow solution of Os($SnMeI_2$)(η^2-S_2CNMe_2)(CO)(PPh_3)$_2$ (0.112 g, 0.090 mmol) in dichloromethane (30 mL) was added 1,2-ethanedithiol (0.30 g, 3.19 mmol) and triethylamine (0.5 mL). The yellow color faded completely in ca. 2 s. After stirring for 1 h the solution was washed with water (3 × 20 mL) and filtered. Addition of ethanol (20 mL) and solvent reduction in vacuo to 5 mL gave a cream precipitate. This was collected by filtration and recrystallized from dichloromethane−ethanol to give pure **7** as a pale microcrystalline solid (0.075 g, 76.9%). Anal. Calcd for $C_{43}H_{43}NOS_4P_2OsSn$·1/3CH_2Cl_2: C, 46.59; H, 3.94; N, 1.25. Found: C, 46.72; H, 3.94; N, 1.41.

Os(Sn[OH]$_3$)(η^2-S_2CNMe_2)(CO)(PPh_3)$_2$ (8). To an orange, stirred solution of Os(SnI_3)(η^2-S_2CNMe_2)(CO)(PPh_3)$_2$ (0.292 g, 0.214 mmol) in benzene−tetrahydrofuran (40−10 mL) was added a solution of KOH (0.661 g, 11.78 mmol) in water (2 mL). The color of the solution faded gradually, and after 25 min all color had gone. The organic layer was washed with

water (3 × 20 mL), filtered, and reduced in vacuo to 2 mL. Addition of hexane (20 mL) precipitated pure **8** as a white microcrystalline solid (0.188 g, 85.0%). Anal. Calcd for $C_{40}H_{39}NO_4P_2S_2SnOs \cdot 1.5CH_2Cl_2$: C, 42.99; H, 3.75; N, 1.32. Found: C, 42.97; H, 3.65; N, 1.21.

Os(Sn[OCH$_2$CH$_2$]$_3$N)(η^2-S$_2$CNMe$_2$)(CO)(PPh$_3$)$_2$ (9). A solution of triethanolamine (1.032 g, 10.2 mmol) in dichloromethane (10 mL) was added to a chilled (0 °C) and stirred solution of Os(SnI_3)(η^2-S_2CNMe_2)(CO)(PPh_3)$_2$ (0.195 g, 0.143 mmol) in dichloromethane (20 mL). The initial yellow color faded totally over 30 min. The reaction was allowed to reach room temperature and was then stirred for a further 30 min. The organic layer was washed with H_2O (3 × 20 mL) and then filtered through paper to remove residual traces of water. Ethanol (20 mL) was added and the solvent volume reduced in vacuo to 5 mL. This gave pure **9** as a white microcrystalline solid (0.111 g, 68.9%). Anal. Calcd for $C_{46}H_{48}N_2O_4P_2S_2SnOs \cdot 1/2CH_2Cl_2$: C, 47.72; H, 4.22; N, 2.39. Found: C, 47.54; H, 4.29; N, 2.35.

Os(Sn[OC(O)CH$_2$]$_3$N)(η^2-S$_2$CNMe$_2$)(CO)(PPh$_3$)$_2$ (10). Os(SnI_3)(η^2-S_2CNMe_2)(CO)(PPh_3)$_2$ (0.105 g, 0.077 mmol) was dissolved in dichloromethane (40 mL), giving an orange solution. To this was added nitrilotriacetic acid (0.043 g, 0.225 mmol) in dichloromethane (10 mL) and triethylamine (0.5 mL). The color of the solution faded totally in ca. 5 s. The resulting colorless solution was stirred for 1 h, then washed with water (3 × 20 mL). The solution was filtered, ethanol (20 mL) added, and the solvent volume reduced in vacuo to 5 mL to give pure **10** as pale yellow microcrystals (0.042 g, 46.6%). Anal. Calcd for $C_{46}H_{42}N_2O_7S_2P_2OsSn \cdot 1/3CH_2Cl_2$: C, 46.45; H, 3.59; N, 2.34. Found: C, 46.17; H, 3.97; N, 2.39.

X-ray Diffraction Studies of 1, 4, 5, 7, and 10. Intensity data were collected using either a Nonius CAD-4 diffractometer (for compound **1**) or a Bruker SMART diffractometer (for compounds **4**, **5**, **7**, and **10**). Data collection covered the unique data set for the CAD-4 and either a sphere or hemisphere for the SMART. Unit cell parameters were from 25 reflections (CAD-4) or all data with $I > 5\sigma(I)$ (SMART). Data were corrected for Lorentz and polarization effects and empirical absorption corrections (ϕ scans for CAD-4 or SADABS for SMART data) applied.

Structure solution was by Patterson and difference Fourier methods, and refinement was by full-matrix least-squares of F^2. All non-hydrogen atoms were allowed to refine anisotropically. Hydrogen atoms were placed geometrically and refined with a riding model with thermal parameters fixed at 20% (50% for methyl groups) greater than the carrier atom. Data collection and refinement parameters are summarized in Table 5.

Programs used for structure solution were SHELXS-97 (G. M. Sheldrick, University of Gottingen, 1997) and SHELXL-97 (G. M. Sheldrick, University of Gottingen, 1997).

Acknowledgment. We thank the Royal Society (London) for a Postdoctoral Fellowship award to T.J.W.

Supporting Information Available: Tables of crystal data, collection and refinement parameters, positional and anisotropic displacement parameters, and bond distances and angles for **1**, **4**, **5**, **7**, and **10**. This material is available free of charge via the Internet at http://pubs.acs.org.

OM990904X